

Crystallization and Electrical Properties of Amorphous Cu-Ag-P Alloys

著者	Shirakawa Kiwamu, Kobayashi Yoshiaki, Masumoto Tsuyoshi
journal or publication title	Science reports of the Research Institutes, Tohoku University. Ser. A, Physics, chemistry and metallurgy
volume	28
number	2
page range	255-265
year	1980-03-29
URL	http://hdl.handle.net/10097/28174

Crystallization and Electrical Properties of Amorphous
Cu-Ag-P Alloys*

Kiwamu Shirakawa**, Yoshiaki Kobayashi** and Tsuyoshi Masumoto

The Research Institute for Iron, Steel and Other Metals

(Received February 29, 1980)

Synopsis

Amorphous Cu-Ag-P alloys (Cu:79~86, Ag:6~14, P:11~14 wt%) were prepared by melt-quenching technique. The crystallization process of these amorphous alloys was examined by electrical resistivity, X-ray diffraction and differential thermal analysis techniques. The T-T-T diagram of the amorphous Cu-Ag-P alloys could be divided into five distinct regions and the electrical resistivity of these alloys decreased in the order of amorphous → metastable-I → supersaturated metastable → metastable-II → stable state.

Compared with traditional strain gauge materials, the present amorphous alloys exhibited a higher gauge factor (1.8~3.1), lower thermal electromotive force relative to copper ($1.07\mu\text{V}/^\circ\text{C}$), comparable specific resistivity at room temperature ($80\mu\Omega\cdot\text{cm}$) and higher negative temperature coefficient of specific resistivity ($-0.7\sim-1.2\times 10^{-4}/^\circ\text{C}$). These values showed to be useful as gauge materials below the crystallization temperature.

I. Introduction

In recent years, a number of amorphous alloys have been prepared by using melt-quenching techniques and their crystallization behavior has been studied in detail⁽¹⁻³⁾. One of authors (T.M.) have indicated that the amorphous phase (Am) transforms to the stable phase (ST) through the formation of two metastable phases (MS-I and MS-II) on heating. Another metastable phase, a supersaturated solid solution (SS) is formed on prolonged aging at lower temperatures. Thus, the crystallization process of amorphous alloys is generally very complex.

* The 1712th report of the Research Institute for Iron, Steel and Other Metals.

** The Research Institute of Electrical and Magnetic Alloys.

On the other hand, it has been known that amorphous alloys have essentially high specific resistivity values ($\sim 10^2 \mu\Omega \cdot \text{cm}$)⁽⁴⁾ and some amorphous alloys show linear change in resistivity below T_x and its temperature coefficient is small ($\sim 10^{-1} \times 10^{-4} / ^\circ\text{C}$)⁽⁴⁾. Therefore, it may be possible to use them for strain gauges. From this point of view, we have tried to search Cu-based amorphous alloys except Cu-Zr alloy known so far, and found that the amorphous alloys are formed in Cu-Ag-P ternary system.

In the present paper, we report the crystallization behavior and the strain gauge characteristics of amorphous Cu-Ag-P alloys. The techniques employed include electrical resistivity, X-ray diffraction and differential thermal analysis.

II. Experimental

Amorphous Cu-Ag-P alloys were prepared by the single-roller type quenching apparatus in the form of ribbons 1~1.5mm wide and 15~20 μm thick. These amorphous ribbons could be prepared only by the iron roller, but not by copper roller for any roll velocity. As the best condition for the formation of amorphous phase, liquid metals (about 800 $^\circ\text{C}$) were ejected at 2~5 kg/cm^2 pressure from the nozzle (0.5~1.0mm diameter) onto the iron roller (20cm diameter) rotating at 2500~5000 r.p.m.. The amorphous nature of the samples was examined by a X-ray monochromator with Mo-K α radiation. Structures of crystal phases appeared after heating were analyzed from X-ray diffraction patterns recorded with Mo-K α radiation. The electrical resistivity was measured by four-point probe method using a potentiometer. The cross-section of the ribbon was estimated from the weight using the specific gravity value of 7.46 g/cm^3 measured for the amorphous $\text{Cu}_{83.5}\text{Ag}_{8.9}\text{P}_{7.6}$ alloy. The differential thermal analysis was performed at a heating rate of 6 $^\circ\text{C}/\text{min}$. The electrical resistivity measurement and differential thermal analysis were carried out under argon atmosphere.

III. Experimental results and discussion

1. Confirmation of the amorphous state

The structure factor ($S(Q)$) was obtained from X-ray diffraction intensity of each amorphous alloy. A sub-peak at about $Q=6 \text{ \AA}^{-1}$ characterized the amorphous alloy. Electron microscopy and electron diffraction pattern also confirmed the amorphous nature of the foil. Hence, we concluded that there were no crystals with grain size greater than

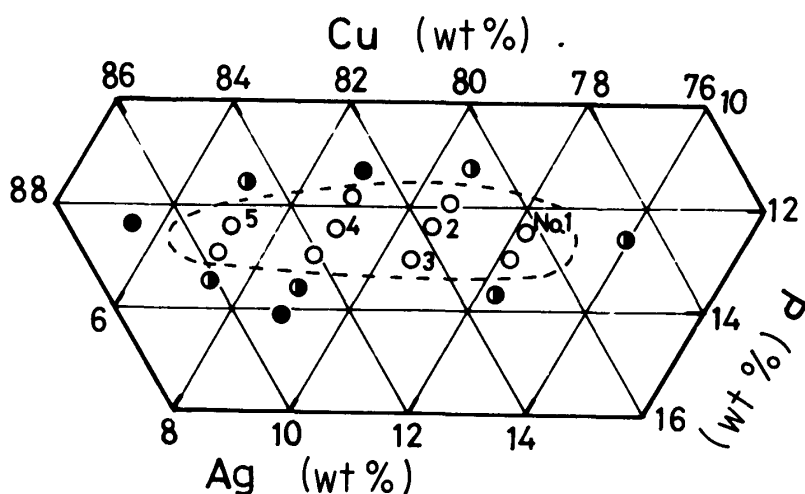


Fig. 1. Composition range of the amorphous Cu-Ag-P alloys.

about 30 Å. The composition range in which the Cu-Ag-P alloys form the amorphous phase is outlined in Fig. 1.

2. Crystallization behavior

Temperature dependence of the electrical resistivity on heating and cooling from liquid nitrogen temperature to 400°C and differential thermal analysis in the temperature range of 20° to 400°C are shown in Fig. 2. Heating rate in both the measurements is 6°C/min. The electrical resistivity curve can be divided into five stages: (1) a linear slight decrease up to about 140°C, (2) drastic decrease (exothermic reaction) between 140~160°C, (3) smooth decrease between 160~200°C, (4) drastic decrease again (exothermic reaction) between 200~220°C, (5) smooth decrease between 220~300°C.

The linear part of first stage below about 120°C is due to no change of amorphous phase (Am). The drastic decrease in the second stage corresponds to the appearance of microcrystals (MS-I) within the amorphous matrix from electron microscopic observation. In the third stage, these microcrystals grow slowly. In the temperature range of the fourth stage, another crystalline phase (MS-II) with X-ray diffraction lines different from those of MS-I phase spreads over all amorphous matrix. In the fifth stage, X-ray diffraction lines became continuously sharper with increasing aging time and new diffraction lines were not observed. Finally the MS-II phase transfers to stable phases (ST) with a small change in electrical resistivity.

In order to follow the crystallization process in detail, changes

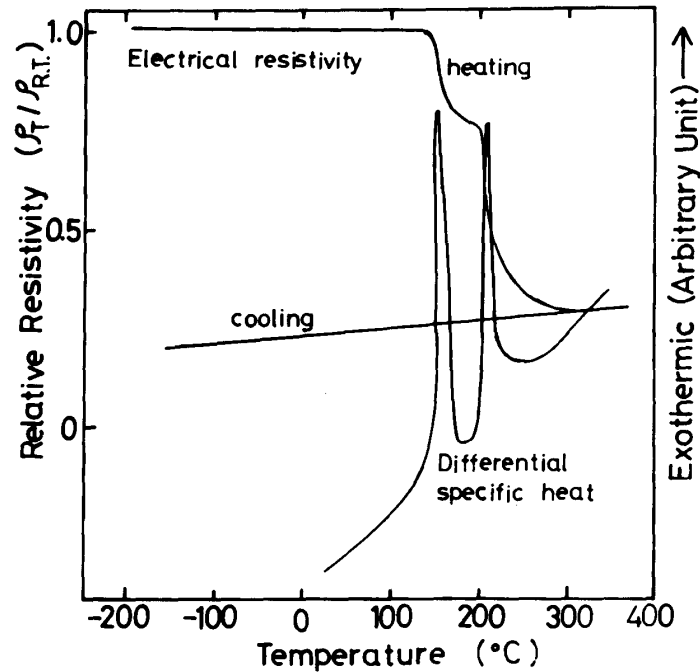


Fig. 2. Curves of relative electrical resistivity and differential thermal analysis at a heating rate of $6^{\circ}\text{C}/\text{min}$ for the amorphous $\text{Cu}_{83.5}\text{Ag}_{8.9}\text{P}_{7.6}$ alloy.

in isothermal electrical resistivity were measured. For example, the aging effect on electrical resistivity at 110, 120, 140, 165 and 290°C is shown in Fig. 3. It is seen in the figure that the values of electrical resistivity in each phase region decreases in the order of $\text{Am} \rightarrow \text{MS-I} \rightarrow \text{MS-II} \rightarrow \text{ST}$. The curve at 120°C shows a slight change in slope at aging time of 10^3 min as shown by an arrow in the figure and the value of electrical resistivity is smaller than that of MS-I phase in the curve at 110°C . As discussed below, this change is due to the appearance of a metastable phase (SS) different from the MS-I.

Then, the temperature dependence of electrical resistivity at different heating rates (5, 20, 40, 50, 70, 120 and $190^{\circ}\text{C}/\text{hr}$) was measured and the result is shown in Fig. 4. The electrical resistivity curves show the transformation of $\text{Am} \rightarrow \text{MS-I} \rightarrow \text{MS-II} \rightarrow \text{ST}$ for high heating rates (120 and $190^{\circ}\text{C}/\text{hr}$), the transformation of $\text{MS-I} \rightarrow \text{SS}$ at point shown by arrows (indicating a change in the temperature coefficient) for intermediate heating rates (40, 50 and $70^{\circ}\text{C}/\text{hr}$) and the transformation of $\text{Am} \rightarrow \text{SS} \rightarrow \text{MS-I} \rightarrow \text{MS-II} \rightarrow \text{ST}$ for low heating rates

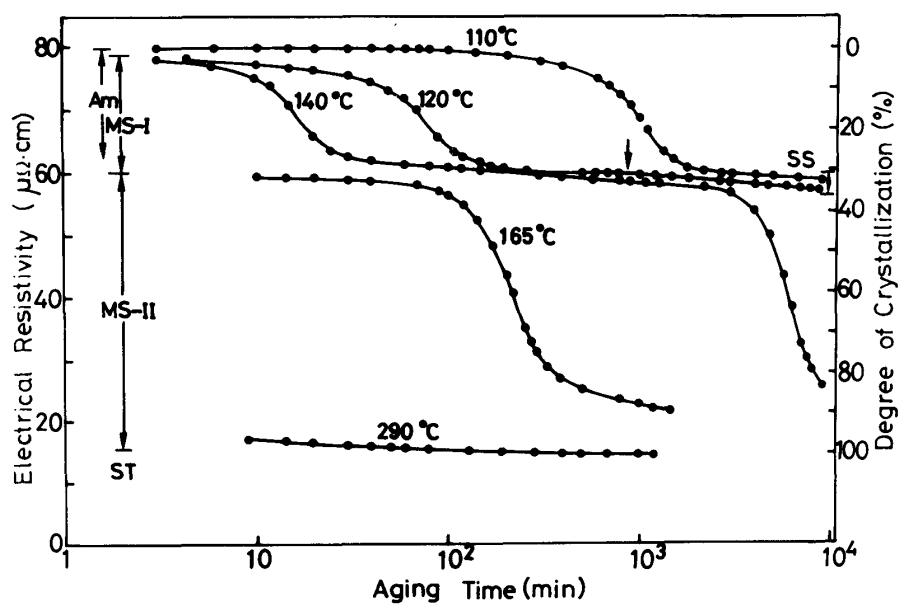


Fig. 3. Changes in electrical resistivity of the amorphous $\text{Cu}_{83.5}\text{Ag}_{8.9}\text{P}_{7.6}$ alloy during aging at 110, 120, 140, 165 and 290°C.

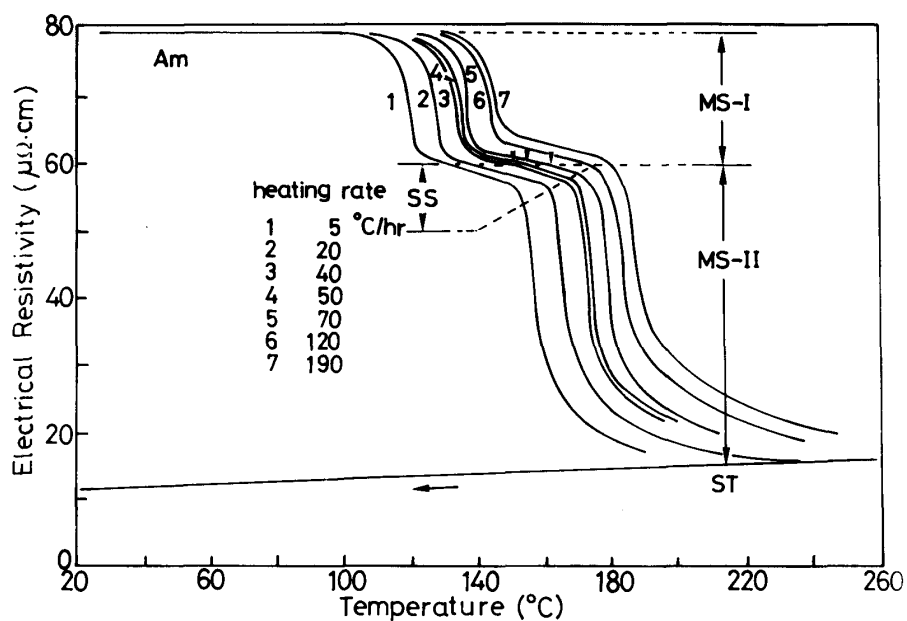


Fig. 4. Changes in electrical resistivity of the amorphous $\text{Cu}_{83.5}\text{Ag}_{8.9}\text{P}_{7.6}$ alloy during heating at the rates of 5, 20, 40, 50, 70, 120 and 190°C/hr.

Table 1. Analysis of X-ray patterns (aged for 1100min at 140°C or 700min at 122°C) showing the presence of metastable phase I (MS-I).

number of line	$d_{\text{obs.}}(\text{Å})$	f.c.c.		f.c.c.	
		hkl	$d_{\text{cal.}}(\text{Å})$	hkl	$d_{\text{cal.}}(\text{Å})$
1	2.363			111	2.361
2	2.098	111	2.090		
3				200	2.045
4	1.821	200	1.810		
5	1.446			220	1.446
6	1.284	220	1.280		
7	1.238			311	1.233
8	1.177			222	1.181
9	1.095	311	1.091		

$a=3.62 \text{ Å}$ $a=4.09 \text{ Å}$

Table 2. Analysis of X-ray diffraction patterns (aged for 6700min at 140°C) showing metastable phase II (MS-II).

number of line	$d_{\text{obs.}}(\text{Å})$	hexagonal hkl	f.c.c.(a) hkl	f.c.c.(b) hkl
1	3.14	111		
2	5.51	112		
3	3.37~2.32 (B)	202	111	
4	2.19	211		
5	2.15			111
6	2.03	300	200	
7	1.98~1.94 (B)	113,212		
8	1.82			200
9	1.76~1.73 (B)	302,104		
10	1.46 (B)	311		
11	1.57	222		
12	1.52	non index		
13	1.45		220	
14	1.41	223		
15	1.37	321		
16	1.33	115		
17	1.30~1.29 (B)	322		220
18	1.23~1.22 (B)	311		
19	1.19~1.15 (B)	323,350,413	222	
20	1.13 (B)	421		
21	1.11~1.09 (B)	206		311
22	1.07~1.05 (B)	422		222

B; broad line

(5 and 20°C/hr).

X-ray diffraction analysis of samples aged for 1100min at 140°C or 700min 122°C is shown in Table 1. This result shows that MS-I phase is a mixture of amorphous and two types of f.c.c. phase ($a=3.62$ and 4.09\AA) and these f.c.c. phases correspond to metallic Cu and Ag respectively. Therefore, the MS-I phase is microcrystals of each metallic element (Cu and Ag), similar to other amorphous alloys. X-ray analysis of the specimen aged for 6700min at 140°C is shown in Table 2, wherein the diffraction lines can be indexed by two different f.c.c. lattices and hexagonal lattice. Table 3. also shows X-ray

Table 3. Analysis of X-ray patterns (aged for 800min at 300°C) showing the presence of stable phase (ST)

number of line	$d_{\text{obs.}}(\text{\AA})$	Cu_3P		Cu		Ag	
		hkl	$d_{\text{cal.}}(\text{\AA})$	hkl	$d_{\text{cal.}}(\text{\AA})$	hkl	$d_{\text{cal.}}(\text{\AA})$
1	3.128	111	3.1268				
2	2.487	112	2.4924				
3	2.363					111	2.3637
4	2.293	202	2.3029				
5	2.169	211	2.1689				
6	2.082			111	2.0831		
7	2.049					200	2.0470
8	2.008	300	2.0074				
9	1.961	113	1.9657				
10	1.926	212	1.9200				
11	1.803			200	1.8040		
12	1.748	302	1.7503				
13	1.709	104	1.7134				
14	1.629	311	1.6265				
15	1.564	222	1.5634				
16	1.441					220	1.4474
17	1.406	223	1.4045				
18	1.359	321	1.3565				
19	1.317	115	1.3142				
20	1.291	322	1.2887				
21	1.276			220	1.2756		
22	1.234					311	1.2344
23	1.220	314	1.2203				
24	1.189	323	1.1915				
25	1.177					222	1.1818
26	1.162	305	1.1645				
27	1.151	413	1.1515				
28	1.126	421	1.1271				
29	1.104	206	1.1079				
30	1.089			311	1.0878		
31	1.071	422	1.0862				
32	1.042			222	1.0415		

$$a=6.954 \text{ \AA}$$

$$c=7.149 \text{ \AA}$$

$$a=3.608 \text{ \AA}$$

$$a=4.089 \text{ \AA}$$

analysis of sample aged for 800min at 300°C. This result shows the presence of 3 phases of Cu, Ag and Cu_3P compound. The result of X-ray analysis for the sample aged for 19700min (2weeks) at 75°C showed to consist of two type of f.c.c. phase, but these diffraction lines were broad. Therefore, the lattice constants of two phases could not be accurately determined. Each phase is in a metastable state supersaturated with phosphorus and appears only for low heating rates or aging at low temperatures.

Based on results of these electrical resistivity and X-ray diffraction analysis, the time-temperature-transformation diagram for amorphous $\text{Cu}_{83.5}\text{Ag}_{8.9}\text{P}_{7.6}$ alloys can be constructed as shown in Fig. 5.

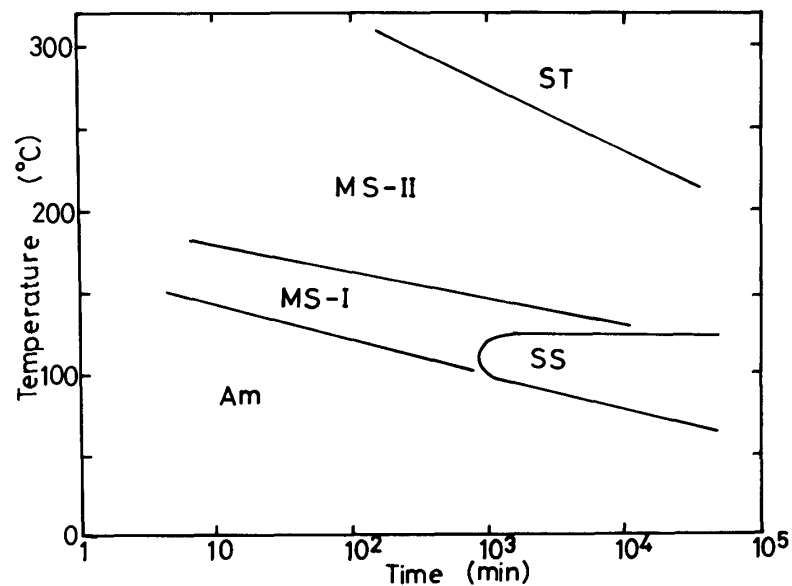


Fig. 5. Time-temperature-transformation diagram of the amorphous $\text{Cu}_{83.5}\text{Ag}_{8.9}\text{P}_{7.6}$ alloy.

3. Electrical properties of the amorphous Cu-Ag-P alloys

In order to evaluate the usefulness of the amorphous alloys as strain gauge materials, their electrical characteristics were measured for five samples of No.1 to No.5 in Fig. 1. Generally, the factors required for good strain gauge materials are (1) high gauge factor (K), (2) low thermo electromotive force relative to copper (e.m.f.), (3) high specific resistivity (ρ) and (4) small temperature coefficient of specific resistivity ($1/\rho(d\rho/dT)$).

Measured values of the above-mentioned four parameters are summarized in Table 4, together with those of traditional strain gauge materials. The $1/\rho(d\rho/dT)$ from room temperature to 100°C is $-0.7 \sim$

Table 4. The values of crystallization temperature, strain gauge factor and electrical properties for five Cu-Ag-P amorphous alloys and two traditional strain gauge alloys.

Alloy No.	Composition(Wt%)			T_x (°C)	K	$\rho(20^\circ\text{C})$ ($\mu\Omega\cdot\text{cm}$)	$C_f(0\sim 40^\circ\text{C})$ ($\times 10^{-4}/^\circ\text{C}$)	$E_{mf}(0\sim 40^\circ\text{C})$ ($\mu\text{v}/^\circ\text{C}$)
	Cu	Ag	P					
1	80.3	12.2	7.5	111	3.1	135.6	-1.23	1.02
2	81.9	10.5	7.6	115	2.5	137.6	-0.97	1.07
3	82.5	10.5	7.0	125	1.8	136.9	-0.90	1.07
4	83.5	8.9	7.6	120	2.4	147.5	-0.67	1.07
5	85.2	7.1	7.7	104	2.8	254.3	-1.00	1.07
Cu _{55~60} Ni _{40~45} Mn _{0~1}					2.04 2.12	45 50	0.2	-45
Ni _{80~85} Cr _{15~20}					2.1 2.65	100 120	0.2	-4

$-1.2 \times 10^{-4}/^\circ\text{C}$ higher than for traditional strain gauge materials, but the specific resistivity of $80 \mu\Omega\text{cm}$ at room temperature is comparable. As shown Fig. 6, the e.m.f. value of $1.07 \mu\text{v}/^\circ\text{C}$ from 0°C to 100°C is very small and is independent of composition.

Next, we obtain the gauge factor K. Generally, electrical resistance R is written as

$$R = \rho(L/S), \quad (1)$$

where L is length, S the cross-section of sample and ρ the specific resistivity. Electrical resistance changes with temperature T and strain ϵ :

$$dR/R = (dR/R)_T + (dR/R)_\epsilon. \quad (2)$$

At constant temperature,

$$dR/R = (dL/L) - (dS/S) + (d\rho/\rho) \quad (3)$$

Since the cross-section changes due to expansion or contraction in one direction by Poisson's ratio ν ,

$$dS/S = -2\nu(dL/L). \quad (4)$$

Hence,

$$(dR/R)/(dL/L) = (1 + 2\nu) + (d\rho/\rho)/(dL/L), \quad (5)$$

where $(dR/R)/(dL/L)$ is gauge factor, K. In amorphous alloys, fracture surface lies at $45\sim 50$ deg. to the tensile axis in the direction of thickness and is perpendicular to direction of the width⁽⁵⁾. Hence, it is thought that ν is about $1/3$. Therefore, the first term of equation (5) becomes about 1.7, and then, the values of K for amorphous alloys are expected to be higher than 1.7 from equation (5).

Now, the relation between dR/R and dL/L was measured. As shown in Fig. 7, dR/R changes linearly with dL/L until the point of tensile fracture of the amorphous alloy. From the slopes of the straight lines, the gauge factors are obtained. The values of K are in the range of 1.8 to 3.1 as shown in Table 4. It is a little higher than for traditional strain gauge materials. From these properties, it appears possible that these amorphous alloys are used as strain gauge materials below their crystallization temperatures.

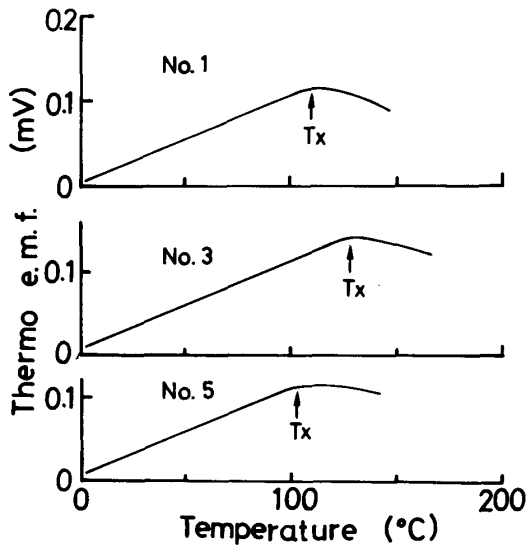


Fig. 6

Fig. 6. Thermo electromotive force against copper for Kinds of amorphous Cu-Ag-P alloys.

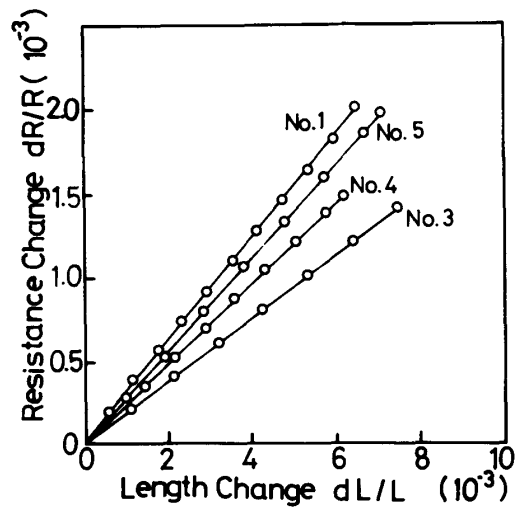


Fig. 7

Fig. 7. Relation between the change of resistance and the length at room temperature for 4 kinds of amorphous Cu-Ag-P alloys.

Summary

Crystallization process and electrical properties of amorphous Cu-Ag-P alloys prepared by the single-roller quenching method were examined using X-ray diffraction, differential thermal analysis and electrical resistivity. The results are summarized as follows:

- (1) Crystallization process is divided into 5 stages. With increasing temperature, the amorphous phase (Am) is crystallized in the sequence of amorphous and two f.c.c. phases (MS-I) \rightarrow two f.c.c. and hexagonal phases (MS-II) \rightarrow Cu, Ag and Cu_3P compound (ST). On the other hand by long aging at lower temperatures, two phases of Cu and Ag supersaturated with P are obtained.
- (2) The electrical resistivity changes linearly with strain until the

point of tensile fracture.

- (3) Compared with traditional strain gauge materials, specific resistivity is a little higher ($-0.7 \sim -1.2 \times 10^{-4} / ^\circ\text{C}$), thermo e.m.f. is lower ($1.0 \mu\text{V}/^\circ\text{C}$), resistivity is comparable ($80 \mu\Omega\text{cm}$) and K is little higher (1.8~3.1) for amorphous Cu-Ag-P alloys. These amorphous alloys may be used for strain gauges at low temperatures.

Acknowledgments

The authors would like to express their sincere thanks to H. Masumoto, President of the Research Institute of Electric and Magnetic Alloys, for helpful discussion and continuous encouragement throughout this work. Thanks are also due to Dr. A. Inoue of the Research Institute for Iron, Steel and Other Metals and Dr. Y. Waseda of the Research Institute of Mineral Dressing and Metallurgy for help in some experiments.

References

- (1) Metallic Glasses, American Society for metals, (1978).
- (2) N.J. Grant and B.C. Giessen, Proc. of 2nd Intern. Conf. on Rapidly Quenched Metals, MIT press (section I) and Meter. Sci. Eng. (sectionII), (1975).
- (3) Proc. of 3rd Intern. Conf. on Rapidly Quenched Metals, Metals Society (London), (1978).
- (4) T.Murata, S. Tomizawa, T. Fukase and T. Masumoto, Scripta Met., 10 (1976), 21.
- (5) For example, S.Tomizawa and T. Masumoto, Sci. Rep. RITU, a26 (1977), 263.